Donor clusters in silicon. Results of ESR measurements

D. New and T. G. Castner
University of Rochester, Rochester, New York 14627
(Received 29 April 1983; revised manuscript received 8 August 1983)

Measurements of ESR spectra of Si:P and Si:As samples with donor concentrations in the range $3\times10^{16}/cm^3$ to $9\times10^{17}/cm^3$ have been obtained in the range 1.4—16 K at 9.5 GHz. The higher temperature $d\chi''/dH$ spectra were integrated to obtain $\chi''(N,T,H)$. The experimental results and simulated spectra based on Poisson statistics, but neglecting cluster topological effects and cluster-cluster interactions, are not in good agreement and demonstrate the problems in using peak heights of the central pair line or triad lines to determine cluster statistics. However, Poisson statistics predictions for the ratio of the integrated intensity of the outer lines to the total integrated intensity are shown to be obeyed and determine the characteristic V_c for cluster formation. $V_c\approx8.2\times10^6$ Å^3 for Si:P and 5.6×10^6 Å^3 for Si:As. A search on a $2.5\times10^{17}/cm^3$ Si:P sample outside the isolated donor transitions for the $\pm5A/6$ hyperfine transitions (A is the Fermi contact hyperfine constant) of the upper $S=\frac{1}{2}$ state of donor triads predicted by Shimizu has revealed very weak extra "bumps" in $d\chi''/dH$ at $H_0\pm35.5$ G in good agreement with Shimizu's prediction. However, the intensity of these "bumps" is very much weaker than expected neglecting topological effects and cluster-cluster interactions. An analysis of the many-electron hyperfine interaction based on a linear combination of Slater determinants is given and applied to the donor triad case. The results are shown to agree with Shimizu's results when overlap terms are neglected. Monte Carlo calculations on donor clusters have yielded the topological distribution function $P(\theta)$ $[\tan(2\theta)=\sqrt{3}(J_{bc}-J_{ac})/(2J_{ab}-J_{bc}-J_{ac})]$ for donor triads and demonstrate it is sharply peaked about $\theta\approx0°$. The role of cluster-cluster interactions on the ESR spectrum of $\chi''(N,T,H)$ is considered and these interactions are discussed for donor triads.

I. INTRODUCTION

Since the discovery of extra ESR transitions associated with shallow donors by Fletcher *et al.*[1] and the subsequent explanation of these extra transitions as donor pair lines by Slichter[2] nearly three decades ago, there has been a substantial revival in interest in donor clusters. For instance, they are the precursors of critical behavior as the insulator-metal transition is approached from the insulating side. In addition, donor pairs, triads, and larger clusters form the basic units of a random spin system (insulating spin-glass) which exhibits spin frustration because of the demonstrated[3] lack of any long-range spin order as the temperature T approaches zero, despite the strong pairwise antiferromagnetic exchange coupling.

Although there have been a significant number of experimental investigations of donor clusters in silicon by ESR (Refs. 4—9) and infrared-optical[10–12] techniques in addition to many theoretical calculations[13–18] of the spin properties and optical properties, a number of questions remain unresolved. These questions concern (1) the unobserved spin transitions predicted by Marko[13] and Shimizu,[14] (2) the origin of the "broad background line" studied by Cullis and Marko,[9] (3) the role of cluster-cluster interactions in addition to the asymmetry effect already considered by Rosso,[15] and (4) the effect of the spin states of pairs on the extra optical transitions (shoulders on the low-energy side of the $1s$-$2p_0$ transition) of donor pairs analyzed in detail by Capizzi *et al.*[12] In addition to these problems there is the question of whether the ESR spectra of donor clusters can be utilized to experimentally test the correctness of the generally assumed random distribution of donors, namely whether the donors obey Poisson statistics. Prior to our work, there had been no serious effort to compare the relative integrated ESR intensities from different size clusters. The early ESR results of Feher *et al.*[4] showed signals from clusters of two, three, and four donors, although the latter were shoulders on the $M_{I_{total}}=\frac{1}{2}$ hyperfine lines resulting from the triad clusters. In many of the early studies the ESR spectra were observed between 4.2 and 1.3 K in the dispersion-derivative mode ($d\chi'/dH$) under strongly saturating, fast-passage conditions. With the objective of obtaining reliable relative intensities of the smaller clusters, we have made slow-passage measurements of the absorption-derivative ($d\chi''/dH$) spectra at sufficiently low power levels to be well below saturation. Another important consideration was to make measurements at sufficiently high temperatures such that kT is much larger than the exchange splittings of the various spin states of a given cluster size so that nearly all of the ESR intensity is recovered from the high-spin states of a given cluster. As the doping level increases, the exchange splittings increase, thus requiring measurements at higher temperatures. The spectra have been integrated twice to obtain the relative contributions to the total integrated intensity from the clusters. The $\chi''(H)$ spectra are compared with calculated spectra based on Poisson statistics, but neglecting topological hyperfine broadening and cluster-cluster interaction effects.

Our own interest on the questions of "extra" or possibly

forbidden transitions arose because of magnetocapacitance measurements[19] which are interpreted in terms of different electrical polarizabilities for the different spin states of a given cluster. This, in turn, led to a novel ESR-capacitance experiment in which one attempts to observe small capacitance shifts as one sweeps through the donor cluster ESR transitions under strongly saturating conditions. This experiment, which has not yet been successful, depends critically on the strength of forbidden ESR transitions between states of different total spin. This situation and the fact that the transitions at $\pm 5A/6$ outside the isolated donor hyperfine transitions (at $\pm A/2$, with A the Fermi-contact hyperfine (hf) constant] predicted by Shimizu[14] had not been observed, led us to search more carefully with extensive signal averaging for the transitions at $\pm 5A/6$. This search did yield weak signals in the vicinity of $\pm 5A/6$ and calculations of triad clusters suggest that the intensity is the right order of magnitude.

The many-electron isotropic hyperfine interaction has been calculated using linear combinations of Slater determinants. A result similar to that usually given[2,4,9,13,14] for pairs is obtained. Neglecting overlap corrections, the results for triads are identical to Shimizu's results.[14] In a related area, there have been recent ESR studies of Na and K trimers and other alkali clusters in an argon matrix.[20,21] In this case the configuration of the three alkali atoms in the trimer is thought to be determined by covalent bonding with a specific configuration energetically favored. For the present case the donors are distributed randomly and clusters of three donors exhibit a topological distribution of triad configurations. Monte Carlo cluster calculations give an indication of the importance of topological hyperfine broadening for triads.

One final objective for the present work was to attempt to learn more about cluster-cluster interactions. The computer-simulated spectra neglecting cluster-cluster interactions and topological hyperfine broadening are shown to be in unsatisfactory agreement with the experimental spectra. Although it has not been possible to quantitatively fit the observed $\chi''(H)$ spectra by incorporating the above two effects, some qualitative conclusions about cluster-cluster interactions can be given.

The background for the ESR of donor clusters is presented in Sec. II. Section III discusses the experimental procedures employed for data acquisition and analysis, while Sec. IV presents and discusses the experimental results. The new development of the many-electron hf interaction is given in Sec. V, followed by a qualitative discussion of cluster-cluster interactions in Sec. VI, and finally by a summary of the important conclusions.

II. BACKGROUND—CLUSTER SPIN STATES

A. Donor pairs

The spin Hamiltonian for donor pairs of spacing $\vec{R}_{ij}$ in a magnetic field $\vec{H}_0$ is given by

$$\mathscr{H}=g\mu_B\vec{H}_0\cdot(\vec{S}_1+\vec{S}_2)+J_{ij}(\vec{R}_{ij})\vec{S}_1\cdot\vec{S}_2+\mathscr{H}_{\rm hf}\,, \tag{1}$$

where $J_{ij}(\vec{R}_{ij})$ is the Heisenberg isotropic exchange interaction [for the many-valley semiconductor Si $J_{ij}=J_{ij}(\vec{R}_{ij},k_0)$ contains interference terms between the different conduction-band minima] and $\vec{S}_1$ and $\vec{S}_2$ are the spins of electrons 1 and 2. $\mathscr{H}_{\rm hf}$ is the hf interaction of the two electrons interacting with the two donor nuclei $\vec{I}_i$ and $\vec{I}_j$ positioned at $\vec{R}_i$ and $\vec{R}_j$. $\mathscr{H}_{\rm hf}$ has traditionally been given as[2]

$$\mathscr{H}_{\rm hf}=A(\vec{S}_1\cdot\vec{I}_i+\vec{S}_2\cdot\vec{I}_j)\,, \tag{2}$$

where A is the isotropic Fermi-contact constant. One notes that $(\vec{S}_1+\vec{S}_2)$ is a good quantum number of (1) when $\mathscr{H}_{\rm hf}$ is neglected. The spin energy levels are shown in Fig. 1 without the contribution from $\mathscr{H}_{\rm hf}$. The form of $\mathscr{H}_{\rm hf}$ in (2) does not commute with $\mathscr{H}-\mathscr{H}_{\rm hf}$ and therefore leads to forbidden transitions for $J_{ij}(\vec{R}_{ij})\gg A$ and to a substantially altered hf spectrum for $J_{ij}(\vec{R}_{ij})\sim A$.[13] Because of the distribution of $\vec{R}_{ij}$ values and the exponential dependence of $J_{ij}(\vec{R}_{ij})$, there will be a broad distribution of J_{ij} values over many orders of magnitude and there will always be some fraction of $J_{ij}(\vec{R}_{ij})$ values close to A.

The form of $\mathscr{H}_{\rm hf}$ given in Eq. (2) states that electron 1 only interacts with nucleus i and electron 2 only interacts with nucleus j. This form is inconsistent with the two-electron wave function for the H_2 molecule independent of whether one employs a Heitler-London wave function or the Hund-Mulliken linear combination of atomic orbitals (LCAO) wave function (or any linear combination of the two). Thus, two donors which form an *isolated* pair in an uncompensated semiconductor should exhibit a hf interaction reflecting the consequences of a H_2-like molecular

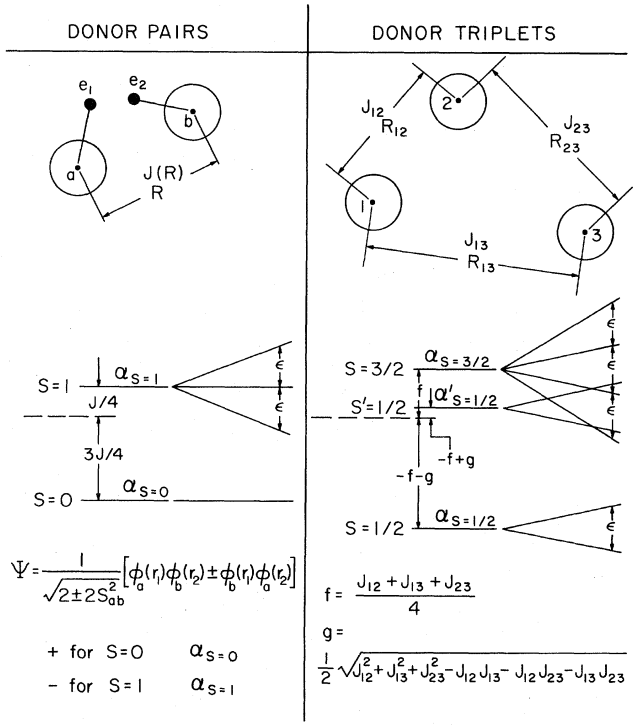

FIG. 1. Energy levels (not including hf interactions) for donor pairs and triads.

wave function for which each electron spends equal time on both nuclei. Neglecting dipolar contributions to $\mathscr{H}_{\rm hf}$ from a small p-state admixture, $\mathscr{H}_{\rm hf}$ should take the form

$$\mathscr{H}_{\rm hf}=\frac{A}{2}(\vec{S}_i\cdot\vec{I}_i+\vec{S}_i\cdot\vec{I}_j+\vec{S}_2\cdot\vec{I}_i+\vec{S}_2\cdot\vec{I}_j)$$
$$=\frac{A}{2}(\vec{S}_1+\vec{S}_2)\cdot(\vec{I}_i+\vec{I}_j)\ . \tag{3}$$

However, this form is only correct within a manifold of states of given S. There will be an off-diagonal term of the form $(A/2)(\vec{S}_1-\vec{S}_2)\cdot(\vec{I}_i-\vec{I}_j)$ between states of different total spin. When this off-diagonal term is taken into account, it leads to the same hf spectrum calculated with $\mathscr{H}_{\rm hf}$ in Eq. (2) and produces the same deviations from the simple hf spectrum (lines at $A/2$, 0, and $-A/2$ with a 1:2:1 intensity ratio) as obtained by Marko.[13] The form given in Eq. (3) for $\mathscr{H}_{\rm hf}$ has also been derived[22] using the Wigner-Eckart theorem within a manifold of states of total spin $S=1$.

B. Donor triads

The spin Hamiltonian for three donors in a cluster has been given by Shimizu[14] and takes the form

$$\mathscr{H}=g\mu_B\vec{H}_0\cdot(\vec{S}_1+\vec{S}_2+\vec{S}_3)+J_{12}\vec{S}_1\cdot\vec{S}_2$$
$$+J_{23}\vec{S}_2\cdot\vec{S}_3+J_{13}\vec{S}_1\cdot\vec{S}_3+\mathscr{H}_{\rm hf}\ , \tag{4}$$

where

$$\mathscr{H}_{\rm hf}=A(\vec{S}_1\cdot\vec{I}_1+\vec{S}_2\cdot\vec{I}_2+\vec{S}_3\cdot\vec{I}_3)$$

is an extension of the form in Eq. (2). $J_{12}(\vec{R}_{12})$, $J_{23}(\vec{R}_{23})$, and $J_{13}(\vec{R}_{13})$ are the three pairwise Heisenberg exchange interactions for the three different pairs. Ignoring $\mathscr{H}_{\rm hf}$, the energy levels for $\vec{H}_0=0$ are given by[14]

$$E_{3/2}=\tfrac{1}{4}(J_{12}+J_{23}+J_{13}),\quad S_{\rm total}=\tfrac{3}{2}\ , \tag{5a}$$

$$E_{1/2}=-\tfrac{1}{4}(J_{12}+J_{23}+J_{13})$$
$$\pm\tfrac{1}{2}(J_{12}^2+J_{23}^2+J_{13}^2-J_{12}J_{23}-J_{12}J_{13}-J_{23}J_{13})^{1/2}\ . \tag{5b}$$

The electron wave functions for these three different spin states are given in Sec. V. The spin energy levels of the donor triad, with the electronic Zeeman effect but without the hf contributions, are shown in Fig. 1. The high-spin $S=\frac{3}{2}$ state is always highest in energy while the two $S=\frac{1}{2}$ states differ in energy depending on the topology of the triad. They are equal in energy for the improbable equilateral triangle ($J_{12}=J_{23}=J_{13}$) with $E_{1/2}=-3J_{12}/4$. However, for the very probable nearly isosceles triangle ($J_{12}\gg J_{23}$ and $J_{13},J_{23}\sim J_{13}$), the two $S=\frac{1}{2}$ states are split by a large amount with the upper $S=\frac{1}{2}$ state being much closer to the $S=\frac{3}{2}$ state than to the lower $S=\frac{1}{2}$ state. A large fraction of the ESR intensity arises from the high-spin state of the donor triad. Thus, to observe all the ESR intensity of donor triads, the high-energy, high-spin state must be fully populated according to Boltzmann statistics, thus requiring $kT\gg\langle J_{12}+J_{23}+J_{13}\rangle/2$. For larger clusters of m donors, the energy of the high-spin state ($S=m/2$) is given by the sum over $m(m-1)/2$ pairwise exchange interaction terms J_{ij}. Since $J_{ij}>0$, the high-spin state energies of larger clusters increase rapidly with m requiring ever larger temperatures to recover all the ESR signal intensity of that cluster size.

Based on the $\mathscr{H}_{\rm hf}$ in Eq. (4), Shimizu has found the hf spectra (see his Table II) for the triad $S=\frac{3}{2}$, and two $S=\frac{1}{2}$ spin states, to be a function of the angle θ where

$$\tan2\theta=\sqrt{3}(J_{23}-J_{13})/(2J_{12}-J_{23}-J_{13})$$

for J_{12}, J_{23}, and $J_{13}\gg A$. His results show the $S=\frac{3}{2}$ state has the standard hf spectrum (lines at $A/2,A/6,-A/6,-A/2$ with a 1:3:3:1 relative intensity ratio). The two $S=\frac{1}{2}$ states exhibit characteristic hf spectra that are, respectively, $(A/2,-A/2)$ with a 4:4 intensity ratio for $S_{1/2l}$ at $\theta=0°$ (also $S_{1/2u}$ at $\theta=30°$) and $(5A/6,A/2,A/6,-A/6,-A/2,-5A/6)$ with a 1:1:2:2:1:1 relative intensity ratio for $S_{1/2u}$ at $\theta=0°$ (also $S_{1/2l}$ at $\theta=30°$). Because $\theta\approx0°$ is highly probable for those many nearly isosceles triangles one might expect to be able to observe the peaks at $\pm5A/6$ predicted by Shimizu.[14] In fact, weak peaks have been observed at the correct positions and are discussed in Sec. IV. Although the same criticism of the $\mathscr{H}_{\rm hf}$ given in Eq. (4) for triads might be made, it can be shown that a many-electron treatment with Slater determinants yields the same result as Shimizu's when overlap terms are neglected. $\mathscr{H}_{\rm hf}$ for triads is discussed in Sec. V.

C. Poisson statistics

Although the basic assumption of Poisson statistics of noninteracting boxes used for noninteracting particles is not strictly valid for donors interacting via the Heisenberg exchange interactions, these interactions are not thought to affect the distribution of donors. Introducing V_c as the characteristic volume of a cluster (box) and $\bar{n}$ as the average number of donors per cluster, then the probability of a cluster (box) containing k donors is $P_k=(\bar{n})^k e^{-\bar{n}}/k!$ The integrated intensity from all spin states in the high-temperature limit from clusters of size k is proportional to the partial susceptibility, i.e., $I_k=\chi_k\propto kP_k$. The total integrated ESR intensity $I_{\rm total}$ from all the clusters will be

$$I_{\rm total}=\sum_{k=1}^{\infty}I_k\propto\sum_{k=1}^{\infty}k\bar{n}^k e^{-\bar{n}}/k!=\bar{n}\propto I_1e^{\bar{n}}\ , \tag{6}$$

where I_1 is the integrated ESR intensity from the isolated donor peaks (at $\pm A/2$ for the P donor; at $\pm3A/2$ for the As donor). The outer peaks also have contributions from the various clusters. These are well approximated by use of the binomial theorem yielding a contribution to the outer peaks of magnitude $I_k/2^{k-1}$. Hence $I_{\rm outer}$ is given by

$$I_{\rm outer}=I_1+\frac{I_2}{2}+\frac{I_3}{4}+\frac{I_4}{8}+\cdots=I_1e^{\bar{n}/2}\ . \tag{7}$$

This leads to the ratio $I_{\rm outer}/I_{\rm total}=e^{-\bar{n}/2}$, which can be readily determined from the experimental data even at doping levels where the individual cluster lines ($k\geq2$) are

no longer resolved. For Si:As the result differs slightly, because the As nucleus has spin $I=\frac{3}{2}$ with a resulting four-line hf spectrum for the isolated donor, and the analysis leads to

$$I_{\text{outer}}/I_{\text{total}}=(\tfrac{1}{2})e^{-3\bar{n}/4}\ .$$

In both cases Poisson statistics predict that the ratio $I_{\text{outer}}/I_{\text{total}}$ decays exponentially with $\bar{n}$. Since $\bar{n}=N_D V_c$, $I_{\text{outer}}/I_{\text{total}}$ will determine the characteristic volume V_c of the size of clusters in the Poisson sense, even though cluster-cluster interactions and topological hf effects smear the spectrum in a complicated manner. As $\bar{n}$ increases beyond 2, cluster-cluster interactions (see Sec. VI) become increasingly important and wipe out the resolution of the individual cluster hf spectra, in addition to altering the spectral shape of a given cluster spectrum. Cluster-cluster interactions are sufficiently important, as will be discussed in Sec. IV comparing experimental spectra and simple calculated spectra ignoring cluster-cluster interactions, that one cannot expect to use the peak heights of particular ESR spectral components of a given cluster to test the applicability of Poisson statistics. The ratio $I_{\text{outer}}/I_{\text{total}}$ defined above does allow one to test the predictions of Poisson statistics in an average sense.

III. EXPERIMENTAL

Measurements of $d\chi''/dH$ have been made at 9.5 GHz with a conventional X-band ESR spectrometer utilizing a Nicolet signal averager in the temperature range 1.4—16 K. The TE_{102}-mode sample cavity was maintained in thermal contact with the liquid-He bath using He exchange gas. Temperatures above 4.2 K were obtained utilizing a wire-wound heater coil wrapped around the cavity. The cavity (sample) temperature was monitored with a calibrated carbon resistor above 4.2 K and with the vapor-pressure—temperature curve of ^{4}He below 4.2 K.

The samples studied and their characteristics are given below in Table I. Both Si:P [float zone (FZ), Czochralski (Cz), and neutron-transmutation-doped (NTD)] and Si:As (FZ and Cz) samples were studied. Donor concentrations of all but the NTD samples (Ref. 23) were determined from room-temperature resistivity measurements. The National Bureau of Standards (NBS) conversion tables between ρ_{RT} and N_D (uncompensated samples) (RT denotes room temperature) for Si:P were employed for both the Si:P and Si:As samples. As a result the true Si:As, N_D values may differ slightly (probably less than 10%) from the values in Table I. The samples were cut with a wafering saw to 1.8×1.0 cm^2 and a thickness between 1 and 4 mm, then handlapped and given a CP-4 etch (1 HF, 1 HNO_3, 1 CH_3COOH).

Because in past studies measurements were usually made of $d\chi'/dH$ in the (1.2—4.2)-K range under strongly saturating adiabatic fast-passage conditions, a power-level dependence of $d\chi''/dH$ was made at each temperature to check for the onset of saturation (for dilute samples $d\chi''/dH$ could only be observed above 4.2 K). The absorption-derivative spectra were taken at power levels well below saturation under slow-passage conditions with 100 Hz field modulation ($\omega_m T_1<1$). The $d\chi''/dH$ spectra, with sufficient sweeps for an adequate signal-to-noise ratio, were integrated to obtain $\chi''(H)$ with the Nicolet signal averager. For a good baseline after the integration it was essential to set the microwave phase accurately and to maintain it with good temperature stability. Integrated intensities of the various cluster lines, as well as the total integrated intensity, were obtained with a planimeter and are accurate to $\pm2\%$.

A careful search was made for the hf lines at $\pm5A/6$ predicted by Shimizu.[14] For the 2.5×10^{17}-cm^{-3} Si:P samples the 25-G region above and below the main hf lines ($\pm A/2$) was averaged over 400 sweeps. A similar search was made for the 1.5×10^{17}-cm^{-3} Si:P sample.[24]

IV. EXPERIMENTAL RESULTS AND DISCUSSION

Figure 2 shows $\chi''(H)$ for the 9×10^{16}-cm^{-3} Si:P (Cz) sample at $T=11$ K. The $4\times$ blowup clearly shows the shoulders on the $k=3$ clusters (at $H_0\pm A/6$) positioned at $\pm A/4$ arising from $k=4$ clusters as reported by Feher *et al.*[4] The dashed curves in Fig. 2 are simulated spectra based on Poisson statistics, the usual degeneracy factors (binomial coefficients—1:2:1 for pairs, 1:3:3:1 for triads, 1:4:6:4:1 for quads, etc.) for the hf line for $M_1=\sum_1^k m_j$, and the same line shape is assumed for each hf line in the spectrum. The line shape has to be fit to a linear superposition of a Gaussian of width ΔH_G and a cutoff Lorentzian of half-intensity at halfwidth ΔH_L given by

$$f(H-H_i)=(1-c)f_G(H-H_i,\Delta H_G)+cf_L(H-H_i,\Delta H_L,A)\ , \tag{8}$$

where the ith hf line is centered at H_i, $c=c(N)$ is a function of doping (the line shape is Gaussian in dilute limit with widths reported by Feher[25]), and the Lorentzian cutoff is arbitrarily taken to have the value of the isolated donor hf splitting A. The constants in (8) were obtained

TABLE I. Sample characteristics (abbreviations as in the text).

Donor, type	ρ_{RT} (Ω cm)	N_D (cm^{-3})	Donor, type	ρ_{RT} (Ω cm)	N_D (cm^{-3})
P, NTD		3×10^{16}	As, FZ	0.067	1.4×10^{17}
P, NTD		6×10^{16}	As, FZ	0.049	2.4×10^{17}
P, Cz	0.090	9×10^{16}	As, FZ	0.035	4.4×10^{17}
P, FZ	0.090	9×10^{16}	As, FZ	0.0263	7.8×10^{17}
P, FZ	0.065	1.5×10^{17}	As, FZ	0.0236	9.6×10^{17}
P, Cz	0.0475	2.5×10^{17}	As, FZ	0.0230	1.0×10^{18}
P, Cz	0.0325	4.8×10^{17}			

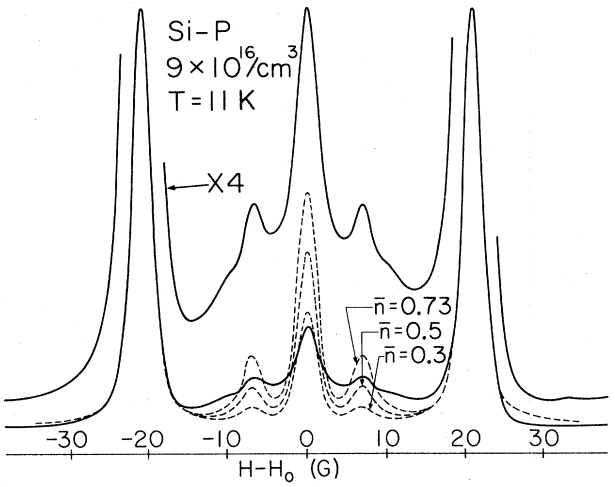

FIG. 2. Si:P $\chi''(H)$ spectrum for a $N_D \approx 9\times 10\text{-cm}^{-3}$ sample. Dashed lines show simulated $\chi''(H)$ spectra based on simple bar spectra, neglecting cluster topological effects and cluster-cluster interactions for $\bar{n}=0.30$, 0.50, and 0.73. The latter value yields the correct value of $I_{\text{outer}}/I_{\text{total}}$.

by fitting the line shape and width of the outer lines (mostly "isolated" donors). The absorption-derivative spectra (not shown) for the more dilute samples ($\bar{n} \leq 2$) did indicate the peak-to-peak widths ΔH_{pp} of $d\chi''/dH$ for the different clusters sized ($k=1$–3) were nearly the same; however, there is no way of experimentally demonstrating whether the tails [from $f_L(H-H_i,\Delta H_L,A)$] are the same. Simulated spectra are shown for $\bar{n}=0.30$, 0.50, and 0.73. The last value is the one that yields the correct value of $I_{\text{outer}}/I_{\text{total}}$ by obtaining the correct integrated area of the cluster portion of the spectrum. The amplitude ratios of the central pair peak and the triad peaks (at $\pm A/6$) to the outer peak are not consistent with a single value of $\bar{n}$. This discrepancy, resulting from topological hf broadening and cluster-cluster interactions, suggests that it is unwise to use relative peak heights to test Poisson statistics or to determine $\bar{n}$. From the data of Cullis and Marko[6] (for a 4×10^{16} cm^{-3} Si:P sample) for $h_{\text{pair}}/h_{\text{outer}}$ (h is the peak height) one would infer a value of $\bar{n}\approx 0.11$ using Poisson statistics. Extrapolating this value to 9×10^{16} cm^{-3} yields a value only about one-third of the value obtained from the present analysis utilizing $I_{\text{outer}}/I_{\text{total}}$.

For more heavily doped Si:P samples ($\bar{n}>2$) the central portion of the cluster spectrum is no longer resolved into separate cluster spectra and is observed to increase relative to the outer hf lines as T is increased. This is illustrated in Fig. 3 for the 4.8×10^{17}-cm^{-3} Si:P sample. Figure 3(a) shows $\chi''(H)$ for several temperatures (different spectra not to the same scale) and 3(b) shows how the average peak height of the two outer lines to the central-line peak height varies with temperature. The higher-energy high-spin states of a given cluster size contribute more to $\chi''(H)$ than do the low-spin states. The enhancement of the central portion of spectra with increasing T results from the increased thermal population of higher-energy spin states.

Figure 4 shows $\chi''(H)$ at $T\approx 16$ for a 1.4×10^{17}-cm^{-3} Si:As sample with several simulated spectra (dashed line) also shown. Again, when the simplifying assumption of identical line shapes is made the relative calculated peak heights differ from the observed $\chi''(H)$. Figure 5 shows results for an intermediate-density 2.5×10^{17}-cm^{-3} Si:P sample. Again the simulated spectra are in poor agreement with the peak heights observed in $\chi''(H)$. The more heavily doped Si:As samples ($N_D \gg 10^{17}$ cm^{-3}) show behavior very similar to that shown in Fig. 3.

Since the use of relative peak heights of different cluster lines is a poor test of Poisson statistics, we have made an analysis based on the ratio of the integrated intensity of the outer hf lines to the total integrated intensity. $I_{\text{total}}=\int_{-\eta A}^{+\eta A}\chi''(H)dH$, where $\eta A\approx 50$ G for Si:P and $\eta A\approx 250$ G for Si:As. The outer lines are assumed symmetric with the line shape as given by Eq. (8). These areas

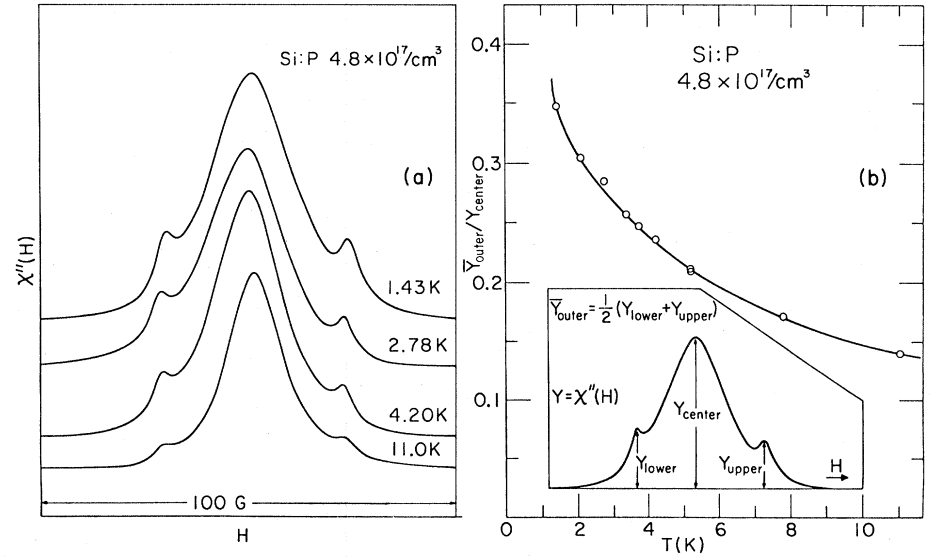

FIG. 3. (a) $\chi''(H)$ for $N_D\approx 4.8\times 10^{17}$-cm^{-3} Si:P samples for four temperatures between $T=1.4$ and 16.3 K. (b) $Y_{\text{outer}}/Y_{\text{center}}$ vs T for the 4.8×10^{17}-cm^{-3} Si:P sample.

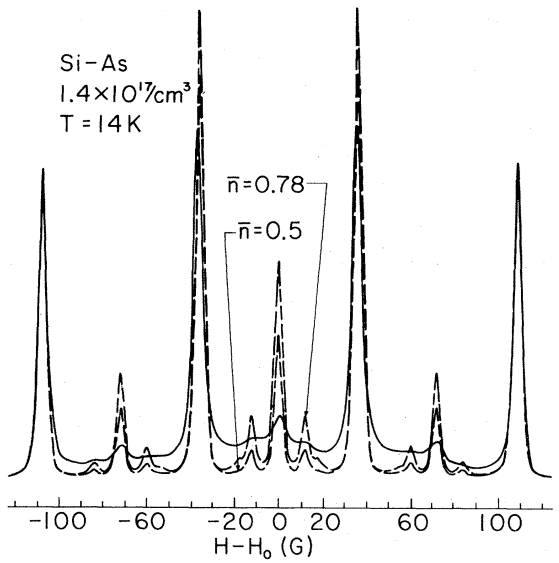

FIG. 4. $\chi''(H)$ at $T \approx 14$ K for a 1.4×10^{17}-cm^{-3} Si:As sample with simulated spectra (dashed line) for several values of $\bar{n}$.

can be determined to within $\pm 2\%$ for the more dilute samples and less accurately for the most heavily doped samples. The $I_{\text{outer}}/I_{\text{total}}$ ratio can be obtained for more heavily doped samples where the central cluster lines are no longer resolved.

$I_{\text{outer}}/I_{\text{total}}$-vs-$N_D$ results for both Si:P and Si:As samples are presented in Fig. 6. The results are consistent with the prediction of Poisson statistics for $I_{\text{outer}}/I_{\text{total}}$ (for Si:P, $I_{\text{outer}}/I_{\text{total}} = e^{-N_D V_c/2}$; Si:As, $I_{\text{outer}}/I_{\text{total}} = \frac{1}{2}e^{-3N_d V_c/4}$) over about 1 order of magnitude in N_D. The slopes in Fig. 6 depend on the characteristic volume V_c and yield 8.2×10^{-18} and 5.6×10^{-18} cm^3 for Si:P and Si:As, respectively (a change in the N_D-vs-ρ_{RT} relationship for Si:As would alter the V_c value for Si:As accordingly). These volumes correspond to critical radii of 125 and 110 Å, respectively. Cullis and Marko obtained a value of 126 Å for Si:P from the susceptibility of the broad-background line which is part of the cluster spectrum. In their theoretical calculations Bhatt and Rice[17] have used a value of $V_c \sim 200 a_B^{*3}$ where a_B^* is the donor effective Bohr radius. The result $V_c = 8.2\times10^{-18}$ cm^3 for Si:P corresponds to a value $V_c \approx 1600 a_B^{*3}$ for $a_B^* = 17.2$ Å [6] for the P donor. This eightfold increase of the experimental value of V_c over that employed in theoretical calculations of clusters could well have implications for the comparison of theory and experiment. However, the V_c determined experimentally is based on the hf spectrum and corresponds to a critical exchange interaction $J_c \approx A$ ($A = 42.6$ G for Si:P).

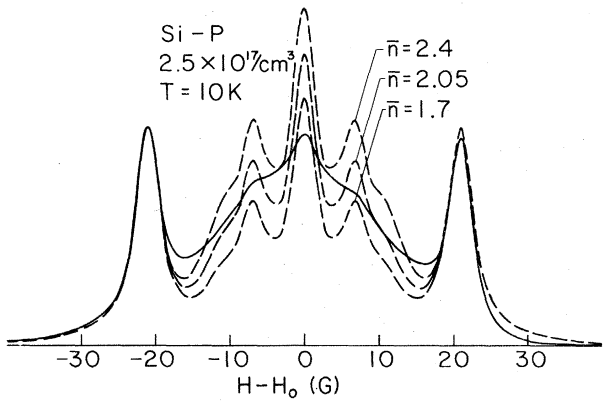

FIG. 5. $\chi''(H)$ for 2.5×10^{17}-cm^{-3} Si:P samples including simulated spectra for different $\bar{n}$ values.

The results in Fig. 6 show that the predictions based on Poisson statistics are correct in an average sense as represented by $I_{\text{outer}}/I_{\text{total}}$. The problem with using peak heights to test Poisson statistics is the presence of several complex broadening mechanisms. These include, for clusters $k \geq 3$, cluster topological hyperfine broadening and cluster-cluster exchange interactions. Based on the simulated pair line being much too big (more than a factor of 2 in Fig. 2) this suggests the latter mechanism may be the more important mechanism. More will be said about the mechanisms in Secs. V and VI.

The prediction by Shimizu[14] of hf lines at $\pm 5A/6$ from donor triads has not been previously reported despite many ESR studies of donor clusters.[24] The results of extensive signal averaging over a 25-G range above and below the outer hf lines at $H_0 \pm A/2$ are shown in Fig. 7. Figure 7(a) shows an enlargement [220× inset in (b), 350 sweeps] of a 25-G range below the main outer line at $H = H_0 - A/2$. A small extra bump is shown centered at -35.5 G below H_0. A similar bump is shown on the negative side of $d\chi''/dH$ centered at $+35.5$ G above H_0 in Fig. 7(b) (365× enlargement of inset, 175 sweeps) with a somewhat poorer signal-to-noise ratio. A subtraction of the smooth tail (using a polynomial fit) of the outer line yields a positive bump of amplitude $0.0012 Y_{pp}^{\text{outer}}$ on the

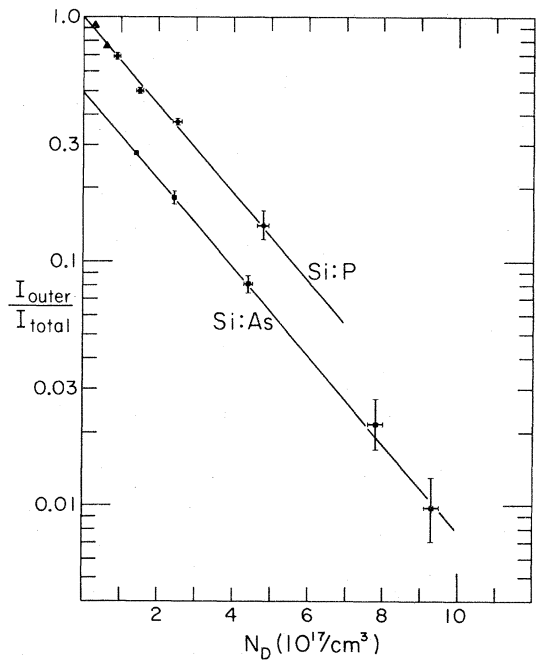

FIG. 6. $I_{\text{outer}}/I_{\text{total}}$ vs N_D for Si:P and Si:As samples. From the result $\bar{n} = N_c V_c$ and the slopes, the characteristic volumes are $V_c = 8.2\times10^{-18}$ cm^3 and $V_c = 5.6\times10^{-18}$ cm^3 for Si:P and Si:As, respectively.

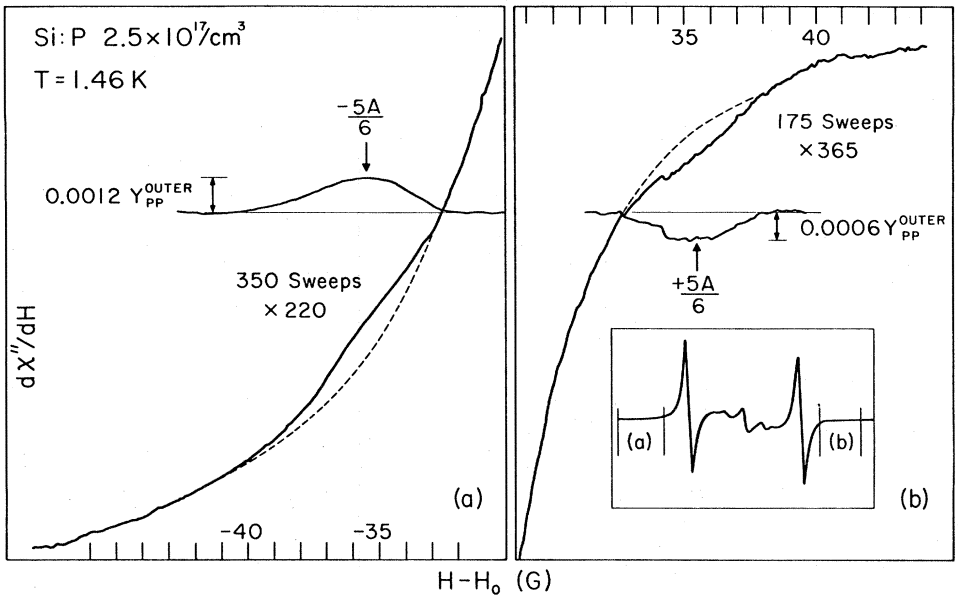

FIG. 7. $d\chi''/dH$ for Si:P sample ($N_D \approx 2.5\times 10^{17}$ cm^{-3}) showing extra absorption at (a) $H_0-35.5$ G and (b) $H_0+35.5$ G. (a) and (b) show a 25-G field range in the vicinity of $\pm 5A/6$ where signal averaging was performed. Inset in (b) shows the overall donor ESR spectra, which is also shown in $d\chi''/dH$ after subtracting the large signal tail from the isolated donors, etc., centered at $\pm A/2$.

low-field side and a negative bump of amplitude $0.0006 Y_{pp}^{\text{outer}}$ on the high-field side. These bumps are not symmetrical about $\pm 5A/6$ and seem to have a tail extending out further than $|5A/6|$ by nearly 5 G. They exhibit the $d\chi''/dH$ shape of a powder pattern characteristic of hf spectra observed in glasses, which is what would be expected for $k=3$ clusters because of the distribution of θ values (see Sec. II B). For this sample $\bar{n}\approx 2$ and a rough estimate yields $Y_{5A/6}(Y_{\text{outer}}^{pp}\times 2)\approx 0.014$ neglecting the $P(\theta)$ distribution, thermal-population factors, overlap effects, and cluster-cluster interactions. These effects all reduce the magnitude of $Y_{5A/6}$ relative to the outer lines and will be considered in Secs. V and VI. This analysis shows the $P(\theta)$ and population factor $f_{1/2u}$ reduce $Y_{5A/6}$ by more than a factor of 2, while overlap and cluster-cluster interactions can account for another substantial reduction. The observation of two bumps very close to $\pm 5A/6$, which are symmetrical about H_0 and have approximately the correct intensity, is strong evidence that these represent the $k=3$ donor cluster hf transitions for the $S_{1/2u}$ state (near $\theta\approx 0°$) predicted by Shimizu.[14]

The $\chi''(H)$ spectra shown in Figs. 2–5 all become asymmetrical at lower temperatures with more absorption on the low-field side of H_0. This asymmetry effect has been studied carefully by Morigaki and Maekawa[8] and our results agree qualitatively. No detailed analysis of the asymmetry effect was made, since it seemed to be well documented and also satisfactorily explained.[15]

V. MANY-ELECTRON hf INTERACTION FOR CLUSTERS

A. Introduction

The electron-spin Hamiltonian represents the interaction between electron spins and the external magnetic field and the hf and quadrupole interactions with nuclei, and, as such, is an average over electron coordinates. Seidel *et al.*[26] have discussed the many-electron hf interaction for an N-center system for the spin state $S=N/2$ using the Slater-determinant approach. When this Slater-determinant approach is applied to the donor cluster, one does not have orthogonal one-electron wave functions on different sites. As discussed by Mattis,[27] this means different Slater determinants ($S_{z_{\text{total}}}=\sum_{i=1}^{k} M_{z_i}$ for a cluster of size k) with the same value of $S_{z_{\text{total}}}$ will not be orthogonal. Furthermore, for the general case with overlap effects, S_{total} will not be a good quantum number for a cluster of arbitrary topology and it will not be possible to write a cluster spin Hamiltonian as a sum of pairwise Heisenberg exchange interactions as in Sec. II. The correct cluster eigenvalues, of course, will be obtained by diagonalizing the $2^k\times 2^k$ matrices of Slater determinants. In the absence of overlap effects, the results will reduce to those discussed in Sec. II. However, the correct form of the many-electron hf spin Hamiltonian will be different for different spin states (different S_{total}) and will also depend on the cluster topology and overlap effects.

B. Donor triads

Because of Shimizu's results[14] and also because of the experimental results shown in Fig. 7, it is worth discussing the $k=3$ cluster case in more detail. There will be a total of eight Slater determinants. Here we shall consider only the three $S_{z_{\text{total}}}=\frac{1}{2}$ states (the $S_{z_{\text{total}}}=\frac{3}{2}$ states are orthogonal to the others; the treatment for the $S_{z_{\text{total}}}=-\frac{1}{2}$ states is the same). The three Slater determinants are

$$\psi_1=(1/6N_1)^{1/2}[(A-F)\beta(1)\alpha(2)\alpha(3)+(B-D)\alpha(1)\alpha(2)\beta(3)+(C-E)\alpha(1)\beta(2)\alpha(3)] , \tag{9a}$$

$$\psi_2=(1/6N_2)^{1/2}[(B-E)\beta(1)\alpha(2)\alpha(3)+(C-F)\alpha(1)\alpha(2)\beta(3)+(A-D)\alpha(1)\beta(2)\alpha(3)] , \tag{9b}$$

$$\psi_3=(1/6N_3)^{1/2}[(C-D)\beta(1)\alpha(2)\alpha(3)+(A-E)\alpha(1)\alpha(2)\beta(3)+(B-F)\alpha(1)\beta(2)\alpha(3)] , \tag{9c}$$

where $A=\psi_a(1)\psi_b(2)\psi_c(3)$, $B=\psi_b(1)\psi_c(2)\psi_a(3)$, $C=\psi_c(1)\psi_a(2)\psi_b(3)$, $D=\psi_c(1)\psi_b(2)\psi_a(3)$, $E=\psi_b(1)\psi_a(2)\psi_c(3)$, and $F=\psi_a(1)\psi_c(2)\psi_b(3)$ are the six permutations of electron orbitals on donor sites a, b, and c of the triad. These electron-permuted orbitals are not orthogonal and the overlap integrals are

$$\langle A\mid B\rangle=\langle B\mid C\rangle=\langle A\mid C\rangle=\langle D\mid E\rangle=\langle D\mid F\rangle=\langle E\mid F\rangle=S_{ab}S_{bc}S_{ac} , \tag{10a}$$

$$\langle A\mid D\rangle=\langle B\mid E\rangle=\langle C\mid F\rangle=S_{ac}^2 , \tag{10b}$$

$$\langle A\mid E\rangle=\langle B\mid F\rangle=\langle C\mid D\rangle=S_{ab}^2 , \tag{10c}$$

$$\langle A\mid F\rangle=\langle B\mid D\rangle=\langle C\mid E\rangle=S_{bc}^2 . \tag{10d}$$

Using (10a) and (10b), one obtains $N_1=1-S_{bc}^2$, $N_2=1-S_{ac}^2$, and $N_3=1-S_{ab}^2$. These three Slater determinants are not orthogonal and one obtains

$$\langle\psi_1\mid\psi_2\rangle=(1/N_1N_2)^{1/2}(S_{ab}S_{bc}S_{ac}-S_{ab}^2)\approx\tfrac{1}{2}(S_{ac}^2+S_{bc}^2)-S_{ab}^2 , \tag{11a}$$

$$\langle\psi_2\mid\psi_3\rangle=(1/N_2N_3)^{1/2}(S_{ab}S_{bc}S_{ac}-S_{bc}^2)\approx\tfrac{1}{2}(S_{ab}^2+S_{ac}^2)-S_{bc}^2 , \tag{11b}$$

$$\langle\psi_1\mid\psi_3\rangle=(1/N_1N_3)^{1/2}(S_{ab}S_{bc}S_{ac}-S_{ac}^2)\approx\tfrac{1}{2}(S_{ab}^2+S_{bc}^2)-S_{ac}^2 . \tag{11c}$$

The treatment by Shimizu[14] only considers electron-spin functions for the Hamiltonian in Eq. (4) and does not take account of overlap. This leads to the three orthogonal linear combinations of Slater determinants (LCSD's) when overlap is neglected, given by

$$\psi_s^{1/2}=(\tfrac{1}{3})^{1/2}(\psi_1+\psi_2+\psi_3) ,$$

$$\psi_e=(\tfrac{1}{6})^{1/2}(\psi_1+\psi_2-2\psi_3) ,$$

and

$$\psi_t^{1/2}=(\tfrac{1}{2})^{1/2}(\psi_1-\psi_2) .$$

For a triad with exhange constants $J_{ab}>J_{bc}>J_{ac}$ and

$$\tan2\theta=\sqrt{3}(J_{bc}-J_{ac})/(2J_{ab}-J_{bc}-J_{ac}) ,$$

the states $\psi_e^{1/2}$ and $\psi_t^{1/2}$ are coupled, leading to the eigenfunctions $\psi_+^{1/2}$ and $\psi_-^{1/2}$ for the upper and lower $S_{\text{total}}=\frac{1}{2}$ states, respectively, given by

$$\psi_+^{1/2}=\cos\theta\psi_e^{1/2}+\sin\theta\psi_t^{1/2} , \tag{12a}$$

$$\psi_-^{1/2}=-\sin\theta\psi_e^{1/2}+\cos\theta\psi_t^{1/2} . \tag{12b}$$

Considering only the Fermi-contact part of the hf interaction [the p admixture is small (less than 2%) for $R/a^*>3.5$] the hf interaction Hamiltonian will be

$$\mathscr{H}_{\text{hf}}=g\mu_B\gamma_p\sum_i^3\sum_\alpha^c\vec{S}_i\cdot\vec{I}_\alpha\delta(\vec{r}_i-\vec{R}_\alpha) , \tag{13}$$

where γ_p is the P nucleus gyromagnetic ratio. The hf interaction for ψ_+ is given by

$$\langle\psi_+^{1/2}\mid\mathscr{H}_{\text{hf}}\mid\psi_+^{1/2}\rangle=\cos^2\theta\langle\psi_e^{1/2}\mid\mathscr{H}_{\text{hf}}\mid\psi_e^{1/2}\rangle+\sin^2\theta\langle\psi_t^{1/2}\mid\mathscr{H}_{\text{hf}}\mid\psi_t^{1/2}\rangle+\sin2\theta\langle\psi_e^{1/2}\mid\mathscr{H}_{\text{hf}}\mid\psi_t^{1/2}\rangle , \tag{14}$$

while $\langle\psi_-^{1/2}\mid\mathscr{H}_{\text{hf}}\mid\psi_-^{1/2}\rangle$ is obtained by replacing θ by $\theta-\pi/2$. The matrix elements in Eq. (14), neglecting overlap corrections and considering only the diagonal first-order terms $S_{zi}I_{z\alpha}\delta(\vec{r}_i-\vec{R}_\alpha)$, are given by

$$\langle\psi_t^{1/2}\mid\mathscr{H}_{\text{hf}}\mid\psi_t^{1/2}\rangle=\frac{A}{2}m_c ,$$

$$\langle\Psi_e^{1/2}\mid\mathscr{H}_{\text{hf}}\mid\psi_e^{1/2}\rangle=\frac{A}{6}[2(m_a+m_b)-m_c] , \tag{15}$$

$$\langle\psi_e^{1/2}\mid\mathscr{H}_{\text{hf}}\mid\psi_t^{1/2}\rangle=\frac{A}{2\sqrt{3}}(m_b-m_a) ,$$

where m_a, m_b, and m_c are the eigenvalues of $I_{z\alpha}$ for the nuclei at a, b, and c. This produces the hf pattern given in Table II of Shimizu.[14] The angular dependence of the lines at $\pm5A/6$ for the $S_{1/2u}$ state is given by $\pm5A/6$ $(1-\frac{8}{5}\sin^2\theta)$. Note that at $\theta=30°$, the maximum value allowed which occurs when $J_{ab}=J_{bc}$ and $J_{ac}=0$, this line has shifted inward to $\pm A/2$ while a pair of the $S_{1/2l}$ lines have shifted outward to $\pm5A/6$. In fact, one observes from Eqs. (14) and (15) that the hf spectra of $S_{1/2u}$ and $S_{1/2l}$ exactly interchange between $\theta=0°$ and 30°.

The hf interaction Hamiltonian of the $S_{\text{total}}=\frac{3}{2}$ state can be shown to be given, neglecting overlap terms, by $(A/3)(\vec{S}_{\text{total}}\cdot\vec{I}_{\text{total}})$ as already alluded to in Sec. II. Neglecting overlap effects, this result for the $S_{\text{total}}=\frac{3}{2}$ state is independent of the topology of the triad. In the high-temperature limit, the $S_{\text{total}}=\frac{3}{2}$ state accounts for $\frac{5}{6}$ of the total intensity from triads. To say more about the intensity of the $S_{1/2u}$ lines at $\pm5A/6$, one needs information on the probability distribution of the θ values for triads.

We have performed Monte Carlo calculations of donors situated on diamond lattice sites in a cubic box approximately 150—175 times V_c containing between 160 and 500 donors depending on N_D. The pairwise exchange interaction $J_{ij}(R_{ij},k_0)$ has been utilized and donors have been grouped into clusters utilizing a cutoff $J_c \approx A = 0.0057$ K (J_c was varied to obtain the correct $\bar{n}$ for the particular Si:P sample; $\bar{n} \sim 2$ for the 2.5×10^{17}-cm^{-3} Si:P sample which yielded the results in Fig. 7). The $P(\theta)$ distribution for triads is shown in Fig. 8 in 2° intervals for $0° < \theta < 30°$. This distribution is sharply peaked near zero with most of the intensity between 0° and 6°. However, there is a relatively flat tail extending all the way to 30°. The small-θ triads come from those triads with $J_{ab} \gg J_{bd}$ and J_{ac}. However, these triads frequently have $J_{ab} \gg kT$ in which case the $S_{1/2u}$ states will not be fully populated. Even for $\theta \approx 30°$ one sometimes has $J_{ab} \approx J_{bc} > kT$ and a resulting reduction of the occupancy of the $S_{1/2u}$ state. Also shown is the quantity $4f_{1/2u}P(\theta)$, with

$$f_{1/2u} = \frac{2e^{-E_{1/2u}/kT}}{2e^{-E_{1/2l}/kT} + 2e^{-E_{1/2u}/kT} + 4e^{-E_{3/2}/kT}} , \tag{16}$$

where the energies are given by Eqs. (5a) and (5b). This quantity is substantially reduced in the $0° < \theta < 2°$ interval to approximately 40% of the $T \to \infty$ value at $T = 1.4$ K. However, this reduction below $P(\theta)$ is not large for $\theta > 4°$. From the results in Fig. 8 we estimate these topological and thermal-population effects reduce the $\pm 5A/6$ hf line intensity by a factor of almost 2 at $T = 1.4$ K for $0° < \theta < 9°$ (which corresponds to a 1.4-G line shift compared to the halfwidth). This still leaves the observed intensity shown in Fig. 7 a factor of 5 smaller than the calculated estimate. Additional reductions can result from overlap effects and cluster-cluster interactions.

It is very difficult to consider overlap effects for a general value of θ, hence we will restrict our consideration to $\theta \approx 0°$ values. For the $S_{1/2u}$ state, the $\pm 5A/6$ lines at $\theta = 0°$ are shifted to

$$\pm A\{\tfrac{5}{6} + \tfrac{2}{3}[S_{ab} - \psi(r_{ab})/\psi(0)]^2 - |\psi(r_{bc})/\psi(0)|^2 - |\psi(r_{ac})/\psi(0)|^2\} . \tag{17}$$

Numerical results from the Monte Carlo calculations for triads using Eq. (17) show that even though the largest S_{ab} obtained can shift the hf line outward as much as 5 G, the predominant effect for most clusters is considerably less than 1 G. Overlap effects cannot account for any significant reduction in the intensity of the $\pm 5A/6$ transitions. The important remaining factor to be considered is the role of cluster-cluster interactions.

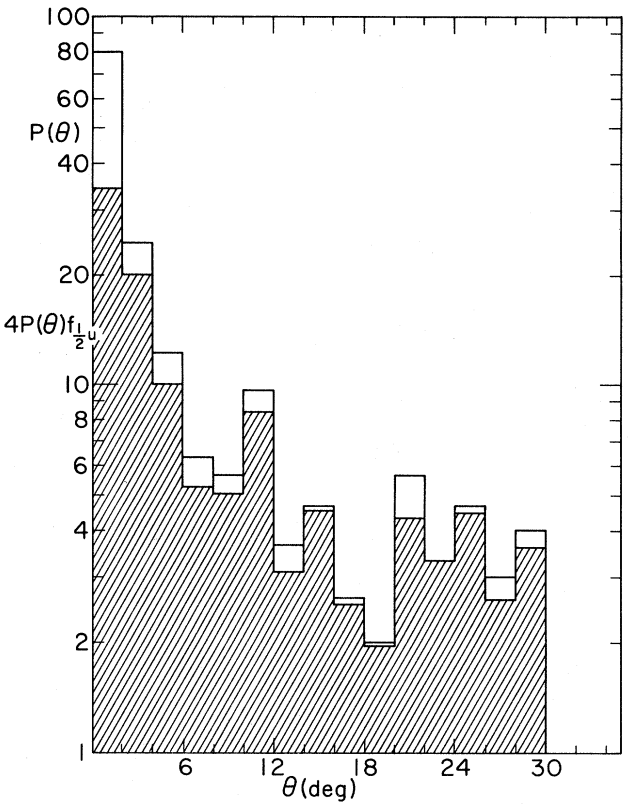

FIG. 8. $P(\theta)$ vs distribution for triads resulting from cluster Monte Carlo calculations. Also shown in the quantity $4P(\theta)f_{1/2u}$ which takes account of the thermal populations of the $S_{1/2u}$ states. This has a substantial effect in the $0° < \theta < 2°$ interval.

VI. CLUSTER-CLUSTER INTERACTIONS

Cluster-cluster interactions result from both residual exchange interactions between donors ($J_{mn} < J_c$) and from dipole-dipole interactions; however, the latter are found to be negligible. With the use of pairwise exchange interactions between all the spins of one cluster with all those of a second cluster, $H_{\rm int}$ takes the form $H_{\rm int} = \Sigma_m \Sigma_n J_{mn} \vec{S}_m \cdot \vec{S}_n$, where m is in cluster I and n in cluster II and $J_{mn} < J_c$. For clusters of size r and s donors, respectively, there will be $r \times s$ different values of J_{mn}. One now needs to combine these terms in terms of the different spin operators for a given cluster. Because of our interest in triads, we will consider triad interactions with isolated donors, pairs, and triads.

For donors 1, 2, and 3 in a triad, and 4 and 5 in a pair, one can show that $H_{\rm int}$ is given by

$$\begin{aligned} H'_{\rm int} = {} & \tfrac{1}{6}(J_{14}+J_{15}+J_{24}+J_{25}+J_{34}+J_{35})(\vec{S}_1+\vec{S}_2+\vec{S}_3)\cdot(\vec{S}_4+\vec{S}_5) \\ & + \tfrac{1}{6}(J_{14}-J_{15}+J_{24}-J_{25}+J_{34}-J_{35})(\vec{S}_1+\vec{S}_2+\vec{S}_3)\cdot(\vec{S}_4-\vec{S}_5) \\ & + \tfrac{1}{12}[J_{14}+J_{15}+J_{24}+J_{25}-2(J_{34}+J_{35})](\vec{S}_1+\vec{S}_2-2\vec{S}_3)\cdot(\vec{S}_4+\vec{S}_5)+\cdots \end{aligned} \tag{18}$$

where the ellipsis represents three more terms in $\vec{S}_1-\vec{S}_2$, $\vec{S}_4-\vec{S}_5$, and $\vec{S}_1+\vec{S}_2-2\vec{S}_3$. The leading term in (18) is a Heisenberg-type term of the form $H_{\rm int}=J_{\alpha\beta}\vec{S}_\alpha\cdot\vec{S}_\beta$, where $\vec{S}_\alpha$ and $\vec{S}_\beta$ are the total spin of the αth and βth clusters, respectively. $J_{\alpha\beta}$ is the sum of all the individual J_{mn}'s. Because the $J_{mn}>0$, the terms involving the Heisenberg interactions of the total spin on each cluster are frequently the largest term; however, because of the very broad distribution in J_{mn} magnitudes and the importance of the interference effects resulting from the many-valley effects, there will in some cases only be a few large J_{mn}'s between any two clusters. Thus, some of the terms in (18) with minus signs will also be large for certain clusters. Terms with spin operators $\vec{S}_1+\vec{S}_2-2\vec{S}_3$, $\vec{S}_1-\vec{S}_2$, and $\vec{S}_4-\vec{S}_5$ limit the lifetimes of the spin states of the individual cluster spin states. The Heisenberg-type terms involving the total spin are diagonal terms that introduce small splitting of the original cluster spin states (i.e., as in Fig. 1).

The consequences of these cluster-cluster residual exchange interactions on the hf interaction are very difficult to consider in any quantitative manner. In principle, one needs to look at the hf interaction of "clusters" of 4, 5, and 6 and/or more donors and look at the hf interaction of these larger clusters as the J_{mn} ($J_{mn}<J_c$) are varied to break the larger cluster into two or more clusters. Qualitatively, the effect of the cluster-cluster interactions is to broaden or washout the hf interaction of a specific small cluster. Qualitatively, the magnitude of the broadening is related to the distribution of the $J_{\alpha\beta}$'s and the other lifetime-limiting terms in (18). Inspection of the results of our Monte Carlo calculations show that the distribution of the $J_{\alpha\beta}$'s is broad between $J\approx A$ and the ESR linewidth ($\Delta H\approx A/15$). Qualitatively, it seems very possible to reduce the intensity of a specific hf line (such as the $\pm 5A/6$ lines of the triad) by a factor of 2—5. A more detailed analysis of this problem will be given in a separate paper.

VII. CONCLUSIONS

The peak heights of the ESR spectra of $\chi''(N,H)$ donor pairs and triads are shown not to be in good agreement with simulated spectra based on Poisson statistics, neglecting topological hf broadening and cluster-cluster interactions. However, the predictions of Poisson statistics for the integrated intensity ratio $I_{\rm outer}/I_{\rm total}$ are obeyed in an average sense over an order of magnitude in donor concentration, namely $I_{\rm outer}/I_{\rm total}$ decays exponentially with donor concentration N_D. From the dependence of $I_{\rm outer}/I_{\rm total}$ on $\bar{n}(N_D)$, the characteristic volume V_c for cluster formation (from Poisson statistics $V_c=\bar{n}/N_D$) is determined. Despite the fact that $I_{\rm outer}/I_{\rm total}$ apparently obeys the Poisson statistics prediction, one should not conclude that the fraction of clusters of a given size ($k\geq 2$) obeys Poisson statistics. In fact, Monte Carlo cluster calculations suggest this is not the case in the $\bar{n}>1$ regime. These calculations, assuming a critical pairwise exchange interaction J_c for a donor to be included in a cluster, show that there are too few pairs and triads and too many large clusters with a small number of improbably very large clusters occurring.

A search for the hf lines at $H_0\pm 5A/6$ for the $S_{1/2u}$-spin state of donor triads predicted by Shimizu has revealed weak "bumps" in $d\chi''/dH$ at $H_0\pm 35.5$ G for a 2.5×10^{17}-cm^{-3} Si:P sample in agreement with Shimizu's prediction. However, the intensity of these bumps relative to the outer line at $\pm A/2$ is more than an order of magnitude smaller than expected, based on Poisson statistics, neglecting overlap effects, topological hf broadening, and cluster-cluster interactions. Topological hf broadening and thermal-population effects can reduce the intensity by, at most, a factor of 2. Since overlap effects at $\theta=0°$ are too small to affect the intensity, most of the intensity reduction must come from cluster-cluster interactions and a smaller fraction of triads than expected from Poisson statistics. The Monte Carlo cluster calculations definitely demonstrate the importance of cluster-cluster interactions in smearing out the cluster hf spectra; however, it is difficult to quantitatively estimate the magnitude of intensity reduction.

The hf spectrum for isolated pairs of donors has deviations from the simple 1:2:1 intensity ratio that result from pairs with $J\approx A$ as calculated by Marko and also from the cluster-cluster interaction and possible deviations from Poisson statistics. The broad-background line discussed by Cullis and Marko results from both topological hf broadening and cluster-cluster interactions of the ESR cluster spectra. Their characteristic radius R_c, determined from the susceptibility associated with the broad-background line, is in excellent agreement with that inferred from the characteristic volume V_c obtained in the present work.

ACKNOWLEDGMENTS

The authors are grateful to Dr. C. Seager of Sandia Laboratories and Dr. J. Cleland of Oak Ridge National Laboratory (ORNL) for providing NTD samples employed in this work. This research was supported in part by the National Science Foundation under Grant DMR-80-07625. One of us (D.N.) is the recipient of a Xerox Corporation Research Fellowship.

[1]R. C. Fletcher, W. A. Yager, G. L. Pearson, A. N. Holden, W. T. Read, and F. R. Merritt, Phys. Rev. 94, 1392 (1954); R. C. Fletcher, W. A. Yager, G. L. Pearson, F. R. Merritt, *ibid.* 95, 844 (1954).

[2]C. P. Slichter, Phys. Rev. 99, 479 (1955).

[3]K. Andres, R. N. Bhatt, P. Goalwin, T. M. Rice, and R. E. Walstedt, Phys. Rev. B 24, 244 (1981).

[4]G. Feher, R. C. Fletcher, and E. A. Gere, Phys. Rev. 100, 1784 (1955).

[5]D. Jérome and J. M. Winter, Phys. Rev. 134, A1001 (1964).

[6]P. R. Cullis and J. R. Marko, Phys. Rev. B 1, 632 (1970).
[7]J. D. Quirt and J. R. Marko, Phys. Rev. B 7, 3842 (1973).
[8]K. Morigaki and S. Maekawa, J. Phys. Soc. Jpn. 25, 912 (1968); 32, 462 (1972).
[9]P. R. Cullis and J. R. Marko, Phys. Rev. B 11, 4184 (1975).
[10]S. Toyotomi, J. Phys. Soc. Jpn. 38, 175 (1975).
[11]P. J. Townsend, J. Phys. C 11, 1481 (1978).
[12]M. Capizzi, G. A. Thomas, F. DeRosa, R. N. Bhatt, and T. M. Rice, Solid State Commun. 31, 611 (1979).
[13]J. R. Marko, Phys. Lett. 27A, 119 (1968).
[14]T. Shimizu, Phys. Soc. Jpn. 25, 1021 (1968).
[15]M. Rosso, J. Phys. Soc. Jpn. 38, 780 (1975).
[16]I. Golka, J. Phys. C 7, L407 (1974); 8, 1443 (1975); Philos. Mag. B 40, 512 (1979).
[17]R. N. Bhatt and T. M. Rice, Philos. Mag. B 42, 859 (1980).
[18]R. N. Bhatt and P. A. Lee, Phys. Rev. Lett. 48, 344 (1982).
[19]D. New, N. K. Lee, H. S. Tan, and T. G. Castner, Phys. Rev. Lett. 48, 1208 (1982).
[20]D. M. Lindsay, D. R. Herschback, and A. L. Kwiram, Mol. Phys. 32, 1199 (1976).
[21]G. A. Thompson and D. M. Lindsay, J. Chem. Phys. 74, 959 (1981).
[22]F. Pake and T. Estle, *The Physical Principles of Electron Paramagnetic Resonance* (Benjamin, Reading, Mass., 1973), p. 175.
[23]These samples, irradiated 21 d (3×10^{16} cm^{-3}) and 42 d (6×10^{16} cm^{-3}) at ORNL, were provided to Dr. C. Seager and one of us (T.G.C.) at Sandia Laboratories by Dr. J. Cleland or ORNL.
[24]In a preliminary account of this work (see D. New and T. Castner, Proceedings of the 16th International Semiconductor Conference, Montpellier, 1982 [Physica (Utrecht) 117B, 128 (1983)]) on a 1.5×10^{17}-cm^{-3} Si:P sample, it was reported that no signal at $H_0\pm5A/6$ was observed to 0.03% of the outer lines at $\pm A/2$. Less signal averaging was utilized and the number of triads was reduced approximately to $\frac{1}{3}$ of those for the 2.5×10^{17}-cm^{-3} Si:P sample.
[25]G. Feher, Phys. Rev. 114, 1219 (1959).
[26]H. Seidel, M. Schwoerer, and D. Schmid, Z. Phys. 182, 398 (1965).
[27]D. Mattis, *The Theory of Magnetism* (Springer, Berlin, 1981), pp. 43—56 and 100—102.